Engineering a Model Protein Cavity to Catalyze the Kemp Elimination

Supplemental Information

Matthew Merski & Brian K. Shoichet*

Dept. of Pharmaceutical Chemistry, University of California, San Francisco

1700 4th St.,

San Francisco, CA 94158-2550

* To whom correspondence should be addressed: shoichet@cgl.ucsf.edu, 415-514-4126

<u>Materials and Methods:</u>

The gene containing T4 phage lysozyme/L99A was subcloned into pET-28 (EMD Biosciences, Darmstadt) and further mutations were generated by overlap extension(1) (Table S4). The plasmids containing the lysozyme constructs were transformed into *E. coli* BL21(DE3) cells and grown in Luria-Bertani media containing kanamycin to O.D.$_{600}$ 0.6 - 0.8 at 37 ºC and then induced with 0.5 mM isopropyl β-D-1-thiogalactopyranoside overnight at 18-20 ºC. The L99A/M102H‡ construct was expressed in Origami 2 (EMD Biosciences, Darmstadt) cells and grown in Terrific broth, otherwise identically to the other constructs. Cells were lysed by microfluidizer, centrifuged at 18,000 x *g* for 45 min and then purified on a nickel-nitrilotriacetic acid column at 4 ºC, pH 6.8 in the presence of 5 mM 2-mercaptoethanol and then dialyzed into 200 mM KCl, 5 mM 2-mercaptoethanol, 0.02% sodium azide, 50 mM phosphate buffer, pH 6.6 once and then two more times in the same buffer without 2-mercaptoethanol or azide and finally concentrated to 10 mg/mL, aliquoted and flash frozen in liquid nitrogen and stored at -80 ºC until needed. Protein purity was ≥95% by SDS-PAGE. Upon thawing the protein was centrifuged to remove precipitate and stored at 4 ºC for up to a week. CD measurements were performed at least in triplicate at pH 5.4 as described(2). pH 5.4 was selected because of the greater refolding of the His-tagged L99A & L99A/M102Q constructs. However, L99A/M102H† and the more advanced constructs did not significantly refold after thermal melting. Briefly, the CD signal was observed at 223 nm with heating, and the resulting thermal melt was fit using the program EXAM(3). ΔCp was set to 10.5 kJ mol^{-1} K^{-1} for all proteins except L99A/M102H†/M106D where ΔCp = 0 kJ mol^{-1} K^{-1}. T$_m$ and ΔH values were used to compare different mutants(4).

The Kemp substrate was synthesized as described(5). Measurements of Kemp eliminase activity were performed at pH 5.0 using a 33 mM succinate, 44 mM imidazole, 44 mM Tris constant ionic strength buffer(6) at 23 °C using an HP8453a spectrophotometer and

observing at 380 nm as described(7). At least four and typically six concentrations of the Kemp substrate between 200 and 800 μM were used in the assays while maintaining a constant 2% concentration of acetonitrile in all assays. Measurements were performed in triplicate on at least two separate days. Assays of the spontaneous rate of the Kemp elimination were measured in triplicate as described previously(7) (Fig. S1-3) The pH-rate profile of the cavity was also performed in the constant ionic strength buffer (Fig. S4). Demonstration of the multiple turnovers of the enzyme (Fig. S7) was accomplished using the normal assay procedure (L99A/M102H†/N68C/A93C, 600 μM Kemp isoxazole, pH 5.0, RT) but the reaction was observed for a much longer time. The absorbance from a spontaneous contemporaneous control reaction was subtracted out and the number of turnovers observed was calculated using the product extinction coefficient (15,800 M^{-1} cm^{-1}) and expressed as a number of turnovers depending on the amount of protein present. The first time point after addition of the enzyme was arbitrarily set to zero to control for absorbance in the buffer not due to the Kemp elimination.

Crystals were grown from a 5 mg/ml solution of the protein by the hanging drop method at 4 ºC over a well solution of 0.1 M sodium acetate, pH 4.5, 30% (w/v) PEG-6000, 0.3 M $LiSO_4$, 3 % trimethylamine *N*-oxide, 50 mM 2-mercaptoethanol, 50 mM 2-hydroxyethyl disulfide. Crystals grew as plates within a month. A fresh well solution with the addition of sucrose to 25% (w/v) served as a cryo solution. Ligands were soaked into the crystals in the cryo solution overnight. Data sets were obtained at the ALS beamline 8.3.1. and have been deposited as PDB ID's 4E97, 4EKP, 4EKQ, 4EKR, & 4EKS. Reflection data were integrated and scaled with XDS(8). Molecular replacement was performed with PHASER(9). Models were refined initially using simulated annealing using PHENIX(10) and COOT(11). The original structure containing 2-mercaptoethanol was refined with anisotropic B-factors, the other models were refined with TLS

B-factors(12). Ligand parameters were generated using PRODRG(13). Complex structures were solved by molecular replacement using the structure of L99A/M102H† in complex with 2-mercaptoethanol (4E97) which was solved by molecular replacement using PDB ID: 181L(14). The models were checked with MolProbity(15). Figures were made with PyMol(16).

Table S1: Specific details of destabilization due to introduced Kemp eliminase mutations. A positive $\Delta\Delta G$ is a stability gain, negative is a stability loss. "Relative to" refers to construct which the current one is compared to in order to calculate $\Delta\Delta G$. Errors are given as the sample standard deviation (± s).

	<Tm> (°C)	<ΔH> (kJ)	<ΔS> (kJ/K)	Relative to	ΔT_m (°C)	$\Delta\Delta G$ (kcal/mol)	k_{cat}/K_M (M^{-1} s^{-1})
L99A	52.8 ±0.2	493.3 ±20.2	1.51	WT	14.4	-5.2	1.7×10^{-2} ±2.1×10^{-3}
L99A/M102Q	44.7 ±0.5	283.7 ±11.2	0.89	L99A	8.1	-1.7	2.6×10^{-1} ±8.5×10^{-2}
L99A/M102Q†	58.2 ±0.2	560.8 ±49.4	1.69	L99A/M102Q	13.4	5.4	6.7×10^{-3} ±5.9×10^{-3}
L99A/M102H†	54.5 ±0.1	431.2 ±36.3	1.32	L99A/M102Q†	3.7	-1.2	4.3×10^{-1} ±1.6×10^{-1}
L99A/M102E†	56.5 ±0.1	464.5 ±24.7	1.41	L99A/M102Q†	1.6	-0.5	1.4×10^{-2} ±1.9×10^{-3}
L99A/M102H†/N68C/A93C	55.3 ±0.2	413.6 ±7.4	1.26	L99A/M102H†	0.8	0.2	1.9×10^{-1} ±9.3×10^{-2}
A99L/M102H†	67.8 ±0.1	592.3 ±51.8	1.74	L99A/M102H†	13.4	5.6	4.9×10^{-2} ±2.1×10^{-3}
L99A/M102H†/M106A	53.9 ±0.1	298.1 ±14.1	0.91	L99A/M102H†	0.6	-0.1	7.7×10^{-1} ±2.3×10^{-1}
L99A/M102H†/M106D	49.6 ±2.0	142.1 ±7.7	0.44	L99A/M102H†	4.9	-0.5	9.2×10^{-1} ±3.0×10^{-1}
L99A/M102H†/L118Q	51.4 ±0.3	287.8 ±13.8	0.89	L99A/M102H†	3.1	-0.7	1.4×10^{0} ±2.9×10^{-1}
L99A/M102H‡	57.3 ±0.2	233.9 ±4.7	0.71	L99A/M102H†/L118Q	5.9	1.0	1.8×10^{0} ±5.7×10^{-2}

Table S2: Table of crystallographic data

Complex	L99A/M102H†/BME	L99A/M102H†/isoxazole	L99A/M102H†/nitrobenzene
PDB entry	4E97	4EKS	4EKP
Data Collection & Processing			
Crystals Used	1	1	1
Wavelength [Å]	1.116	1.116	1.116
Space Group	P2$_1$	P2$_1$	P2$_1$
Unit Cell Parameters			
a, b, c [Å]	48.30, 75.42, 52.60	48.30, 75.37, 52.65	48.37, 75.53, 52.72
α, β, γ [°]	90.00, 93.40, 90.00	90.00, 93.15, 90.00	90.00, 93.22, 90.00
Matthews Coefficient[Å^3/Da]	2.24	2.24	2.25
Solvent Content [%]	45.1	45.1	45.4
Diffraction Data			
Resolution Range [Å]	50-1.30 (1.36-1.30)	50-1.64 (1.73-1.64)	50-1.64 (1.73-1.64)
Unique Reflections	92,251 (11,609)	43,970 (6,644)	45,872 (6,794)
R(I)sym [%]	5.4 (48.7)	5.2 (31.3)	4.6 (33.5)
Completeness [%]	99.9 (99.8)	95.2 (97.8)	98.8 (99.1)
Redundancy	6.4 (3.6)	2.6 (2.6)	2.5 (2.5)
I/σ(I)	19.18 (2.81)	14.2 (3.0)	15.9 (3.0)
Refinement			
Resolution Range [Å]	48.2-1.30	48.2-1.64	43.2-1.64
Reflections Used (work/free)	88,561/3,690	42,189/1,771	44,024/1,839
Final R Values (work/free)[%]	14.20/16.55	17.13/19.80	16.94/19.63
Protein Residues	353	349	349
Ligand Atoms	4	9	9
Water Molecules	413	315	336
RMSDs			
Bonds[Å]	0.014	0.010	0.008
Angles[º]	1.48	1.2	1.1
Ramachandran plot: residues in:			
Favored (98%) regions [%]	99.7	99.2	99.5
Allowed (>99.8%) regions [%]	100.0	100.0	100.0
Mean B-Factor [Å^2]			
Protein	13.4	14.9	16.1
Ligand	24.8	25.7	18.3
Water Molecules	23.9	24.9	26.3

Table S2: Table of crystallographic data (con't)

Complex	L99A/M102H†/2-cyanophenol	L99A/M102H†/4-nitrophenol
PDB entry	4EKR	4EKQ
Data Collection & Processing		
Crystals Used	1	1
Wavelength [Å]	1.116	1.116
Space Group	$P2_1$	$P2_1$
Unit Cell Parameters		
a, b, c [Å]	48.17, 75.63, 52.80	48.21, 76.07, 52.81
α, β, γ [°]	90.00, 93.21, 90.00	90.00, 93.01, 90.00
Matthews Coefficient[Å^3/Da]	2.25	2.26
Solvent Content [%]	45.3	45.7
Diffraction Data		
Resolution Range [Å]	50-1.49 (1.57-1.49)	50-1.54 (1.62-1.54)
Unique Reflections	57,470 (8,557)	52,590 (7,600)
R(I)sym [%]	4.6 (33.2)	4.3 (33.7)
Completeness [%]	93.1 (95.8)	93.4 (96.3)
Redundancy	2.7 (2.6)	2.7 (2.6)
I/σ(I)	15.1 (3.1)	15.7 (3.1)
Refinement		
Resolution Range [Å]	48.1-1.49	48.1-1.54
Reflections Used (work/free)	55,185/2,277	50,467/2,116
Final R Values (work/free)[%]	18.19/20.58	17.51/20.41
Protein Residues	349	349
Ligand Atoms	9	10
Water Molecules	308	295
RMSDs		
Bonds[Å]	0.014	0.021
Angles[º]	1.5	1.8
Ramachandran plot: residues in:		
Favored (98%) regions [%]	99.2	99.2
Allowed (>99.8%) regions [%]	100.0	100.0
Mean B-Factor [Å^2]		
Protein	14.2	16.9
Ligand	15.7	14.4
Water Molecules	23.6	27.3

Table S3: Comparison of different approaches towards engineering improved catalysts for the Kemp elimination. Parenthetical values in the "Catalysis" column refer to activities gained from applying directed evolution to designed enzymes. The catalytic improvement of Kemp catalytic antibodies is estimated from the slope (2×10^{-5} s^{-1} pH^{-1}) of the line from figure S3. The catalytic improvement for the enzymes from this report compares the measured k_{cat}/K_M at pH = 5.0 for the most active construct L99A/M102H‡ while the higher pH ~ 7.3 uses the rate measurement at pH 7.3 for the less designed L99A/M102H†/N68C/A93C in the constant ionic strength buffer with the reported spontaneous rate from ref. 7 using acetate buffer at pH 7.25 to compare the results from this report to the values from the other previously reported designed Kemp eliminases.

	Catalysis (k_{cat}/K_M) (M^{-1} s^{-1})	Catalytic Improvement $[(k_{cat}/K_M)/k_{uncat}]$	pH Optimum (catalytic residue)
Catalytic Antibodies(17)	5,500	~5×10^9 (pH 7.5)	pH > 7.0 (glutamate)
Computational Design (MD)(18)	425	4×10^8 (pH 7.25)	pH = 7.0 (aspartate)
Computational Design [Rosetta, KE70 (directed evolution)](19)	126 (54,800)	1×10^8 (5×10^{10}) (pH 7.25)	pH > 7.0 (His-Asp dyad)
Computational Design [Rosetta, KE07 (directed evolution)](7, 20)	12.2 (2,600)	1×10^7 (2×10^9) (pH 7.25)	pH > 7.0 (glutamate)
Computational Design [Rosetta, KE59 (directed evolution)](7, 21)	~160 (60,430)	1×10^8 (5×10^{10}) (pH 7.25)	pH > 7.0 (glutamate)
Computational Design (Rotamer minimization) (22)	5.8	3×10^5 (pH 8.0)	pH > 8.0 (glutamate)
This paper	1.8	7×10^7 / 3.2×10^5 (pH 5.0 / ~7.3)	pH = 5.0 (histidine)

Table S4: Amino acid sequences of designed proteins reported in this study

```
>T4 Lysozyme NHis L99A
MGSSHHHHHHSSGLVPRGSHMNIFEMLRIDEGLRLKIYKDTEGYYTIGIGHLLTKSPSLNAAKSELDKAIGRNCNGVITKDEAEKLFNQDVDAAVRGILRNAKLKPVY
DSLDAVRRCAAINMVFQMGETGVAGFTNSLRMLQQKRWDEAAVNLAKSRWYNQTPNRAKRVITTFRTGTWDAYKNL*
>T4 Lysozyme NHis L99A/M102Q
MGSSHHHHHHSSGLVPRGSHMNIFEMLRIDEGLRLKIYKDTEGYYTIGIGHLLTKSPDLNAAKSELDKAIGRNCNGVITKDEAEKLFNQDVDAAVRGILRNAKLKPVY
DSLDAVRRCAAINQVFQMGETGVAGFTNSLRMLQQKRWDEAAVNLAKSRWYNQTPDRAKRVITTFRTGTWDAYKNL*
>T4 Lysozyme NHis L99A/M102Q†
MGHHHHHHDYDIPTTENLYFQGSMNIFEMLRIDEGLRLKIYKDCEGYYTIGIGHLLTKSPDLNAAKSELDKAIGRNCNGVITKDEAEKLFNQDVDAAVRGILRNAKL
KPVYDSLDAVRRCAAINQVFQMGVTGVAGFTNVLRMLQQKRWDEAAVNLAKSRWYNQCPDRAKRVITTFRTGTWDAYKNL*
>T4 Lysozyme NHis L99A/M102H†
MGHHHHHHDYDIPTTENLYFQGSMNIFEMLRIDEGLRLKIYKDCEGYYTIGIGHLLTKSPDLNAAKSELDKAIGRNCNGVITKDEAEKLFNQDVDAAVRGILRNAKL
KPVYDSLDAVRRCAAINHVFQMGVTGVAGFTNVLRMLQQKRWDEAAVNLAKSRWYNQCPDRAKRVITTFRTGTWDAYKNL*
>T4 Lysozyme L99A/M102E†
MNIFEMLRIDEGLRLKIYKDCEGYYTIGIGHLLTKSPDLNAAKSELDKAIGRNCNGVITKDEAEKLFNQDVDAAVRGILRNAKLKPVYDSLDAVRRCAAINEVFQMG
VTGVAGFTNVLRMLQQKRWDEAAVNLAKSRWYNQCPDRAKRVITTFRTGTWDAYKNL*
>T4 Lysozyme NHis A99L/M102H†
MGHHHHHHDYDIPTTENLYFQGSMNIFEMLRIDEGLRLKIYKDCEGYYTIGIGHLLTKSPDLNAAKSELDKAIGRNCNGVITKDEAEKLFNQDVDAAVRGILRNAKLK
PVYDSLDAVRRCALINHVFQMGVTGVAGFTNVLRMLQQKRWDEAAVNLAKSRWYNQCPDRAKRVITTFRTGTWDAYKNL*
>T4 Lysozyme NHis L99A/M102H†/N68C/A93C
MGHHHHHHDYDIPTTENLYFQGSMNIFEMLRIDEGLRLKIYKDCEGYYTIGIGHLLTKSPDLNAAKSELDKAIGRNCNGVITKDEAEKLFCQDVDAAVRGILRNAKLK
PVYDSLDCVRRCAAINHVFQMGVTGVAGFTNVLRMLQQKRWDEAAVNLAKSRWYNQCPDRAKRVITTFRTGTWDAYKNL*
>T4 Lysozyme NHis L99A/M102H†/M106A
MGHHHHHHDYDIPTTENLYFQGSMNIFEMLRIDEGLRLKIYKDCEGYYTIGIGHLLTKSPDLNAAKSELDKAIGRNCNGVITKDEAEKLFNQDVDAAVRGILRNAKL
KPVYDSLDAVRRCAAINHVFQAGVTGVAGFTNVLRMLQQKRWDEAAVNLAKSRWYNQCPDRAKRVITTFRTGTWDAYKNL*
>T4 Lysozyme NHis L99A/M102H†/M106D
MGHHHHHHDYDIPTTENLYFQGSMNIFEMLRIDEGLRLKIYKDCEGYYTIGIGHLLTKSPDLNAAKSELDKAIGRNCNGVITKDEAEKLFNQDVDAAVRGILRNAKL
KPVYDSLDAVRRCAAINHVFQDGVTGVAGFTNVLRMLQQKRWDEAAVNLAKSRWYNQCPDRAKRVITTFRTGTWDAYKNL*
>T4 Lysozyme NHis L99A/M102H†/L118Q
MGHHHHHHDYDIPTTENLYFQGSMNIFEMLRIDEGLRLKIYKDCEGYYTIGIGHLLTKSPDLNAAKSELDKAIGRNCNGVITKDEAEKLFNQDVDAAVRGILRNAKL
KPVYDSLDAVRRCAAINHVFQMGVTGVAGFTNVQRMLQQKRWDEAAVNLAKSRWYNQCPDRAKRVITTFRTGTWDAYKNL*
>T4 Lysozyme NHis L99A/M102H‡
MGHHHHHHDYDIPTTENLYFQGSMNIFEMLRIDFGLRLKIYKNCEGYYTIGIGHLLTKSPDLNAAKSELDKAIGRNCNGVITKDEAEKLFNQDVDAAVRGILRNAKL
KPVYDSLDAVRRCAAINHVFQDGVTGVAGFTNVQRMLQQKRWDEAAVNLAKSRWYNQCPDRAKRVITTFRTGTWDAYKNL*
```

Table S5: Ranking of important molecules by molecular docking. A set of ~656,000 were docked against PDB ID 4E97 as described in the methods. The small molecule neutral analogs of the reaction that were observed in the crystal structures scored well, all being in the top 1% of the list. The actual Kemp substrate did not rank as well but was nevertheless in the top 4% of the database while the product was ranked poorly, which would be beneficial to the reaction. RMSD's are calculated from the highest DOCK ranked pose. The RMSD of the Kemp substrate is calculated from the nine common atoms it shares with 1,2-benzisoxazole (PDB 4EKS), while that of the product is calculated from the 10 common atoms shared with 4-nitrophenol (PDB 4EKQ).

Ligand	DOCK Rank (% of database)	DOCK Score (kcal/mol)	RMSD (Å)
nitrobenzene	713 (0.11)	-16.88	0.64
1,2-benzisoxazole	867 (0.13)	-16.59	3.47
2-cyanophenol	2,854 (0.44)	-14.15	0.75
4-nitrophenol	6,373 (0.97)	-11.81	0.76
Kemp substrate	24,423 (3.72)	-3.39	3.47
Kemp product	92,358 (14.08)	25.00	2.64

Figure S1: The change in absorbance at 380 nm over time due to the spontaneous Kemp elimination in the constant ionic strength buffer used for enzymatic assays. Assays performed at pH 5.0 with an initial isoxazole concentration of 0.2 mM. 1X buffer is 33 mM succinate, 44 mM imidazole and 44 mM Tris(6). Assays performed as described previously(7).
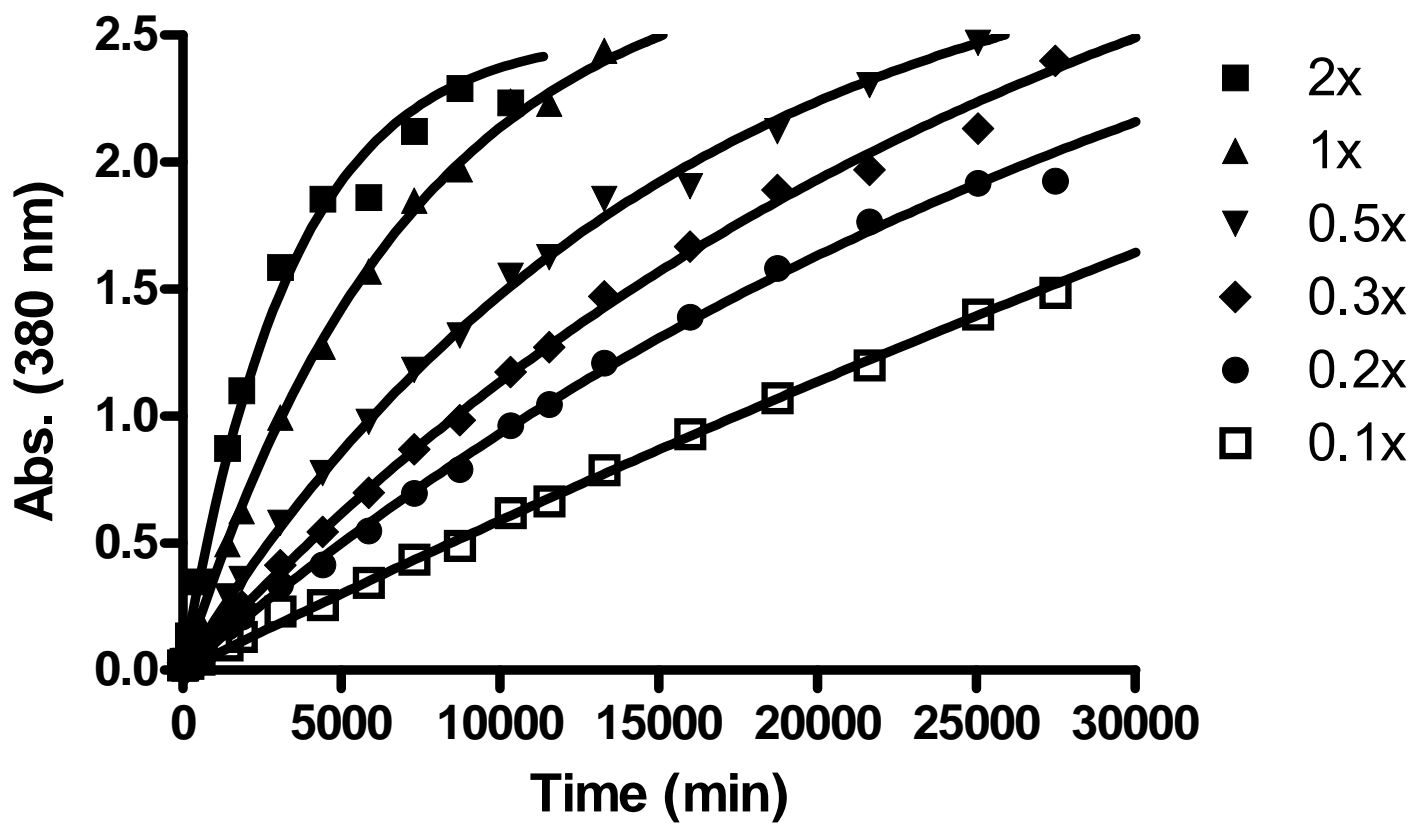
Figure S2: The effect of buffer concentration on the rate of the spontaneous Kemp elimination using the same constant ionic strength buffer for the enzymatic activity assays used in this report. Assay was performed at 23 °C at pH 5.0 with 0.2 mM Kemp substrate. Analysis as described previously(7). The slope of the fit line is 1.5×10^{-6} min^{-1} mM^{-1}
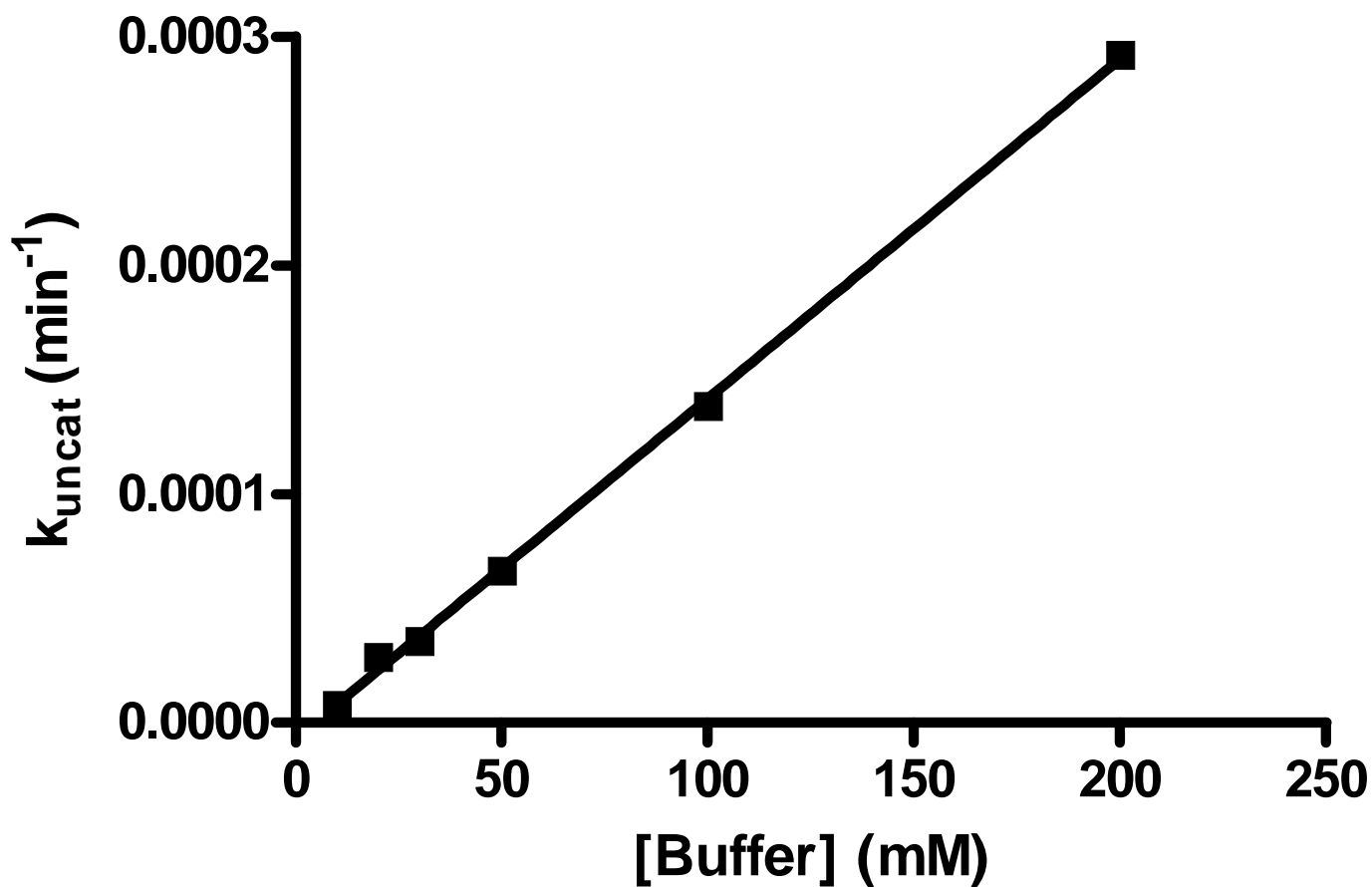
Figure S3: Comparison of the reported spontaneous rates of the Kemp elimination at different pH values. The values represented by colored icons were determined for this report, the other values are as reported in the literature(7). The fit line for the spontaneous rate of Kemp elimination was calculated using the rate measured at pH 5.0 in the constant ionic strength buffer and the literature values from reference 7. The slope of the fit line is 2×10^{-5} s^{-1} pH^{-1}. The rate of spontaneous decomposition in the constant ionic strength buffer was 2.45×10^{-8} s^{-1} at pH 5.0 and 1.24×10^{-7} s^{-1} at pH 7.25. In imidazole buffer the rate of spontaneous decomposition was 1.42×10^{-7} s^{-1} at pH 7.3.
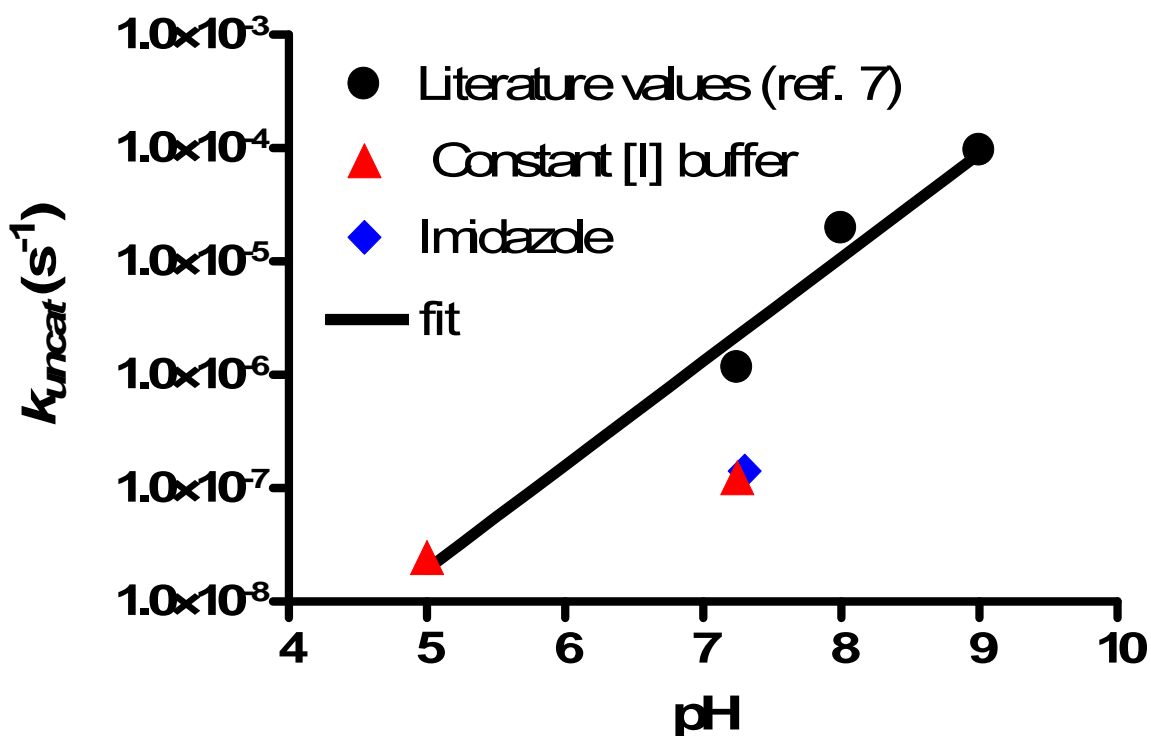
Figure S4: The effect of pH on the rate of the Kemp elimination at 23 °C catalyzed by L99A/M102H†/N68C/A93C using a constant ionic strength buffer(6). Note that the data are scattered around an average k_{cat}/K_M value of 0.37 ±0.15 without significant change or noticeable slope. The pK_a of His102 is likely well below pH 5.0. Note that the Y-axis is on a log scale.
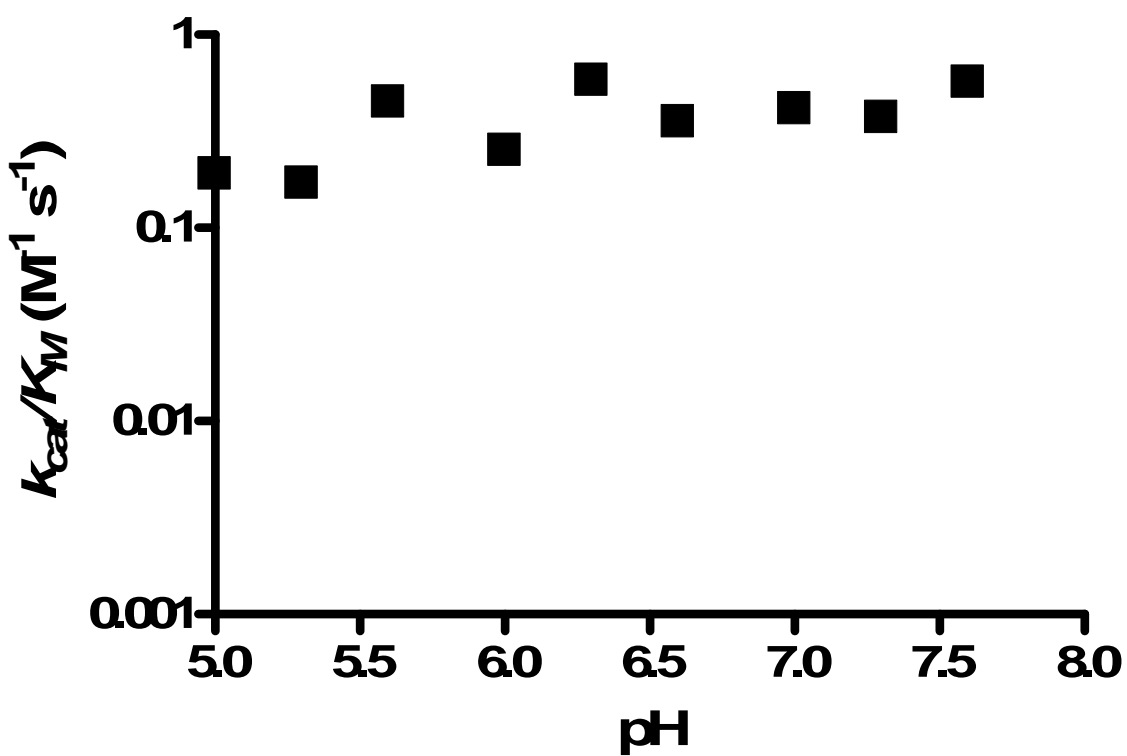
Figure S5: Illustrative example of catalysis of the Kemp elimination by several of the constructs described in this work. Data points are the average of triplicate measurements and the endogenous rate has been subtracted out.
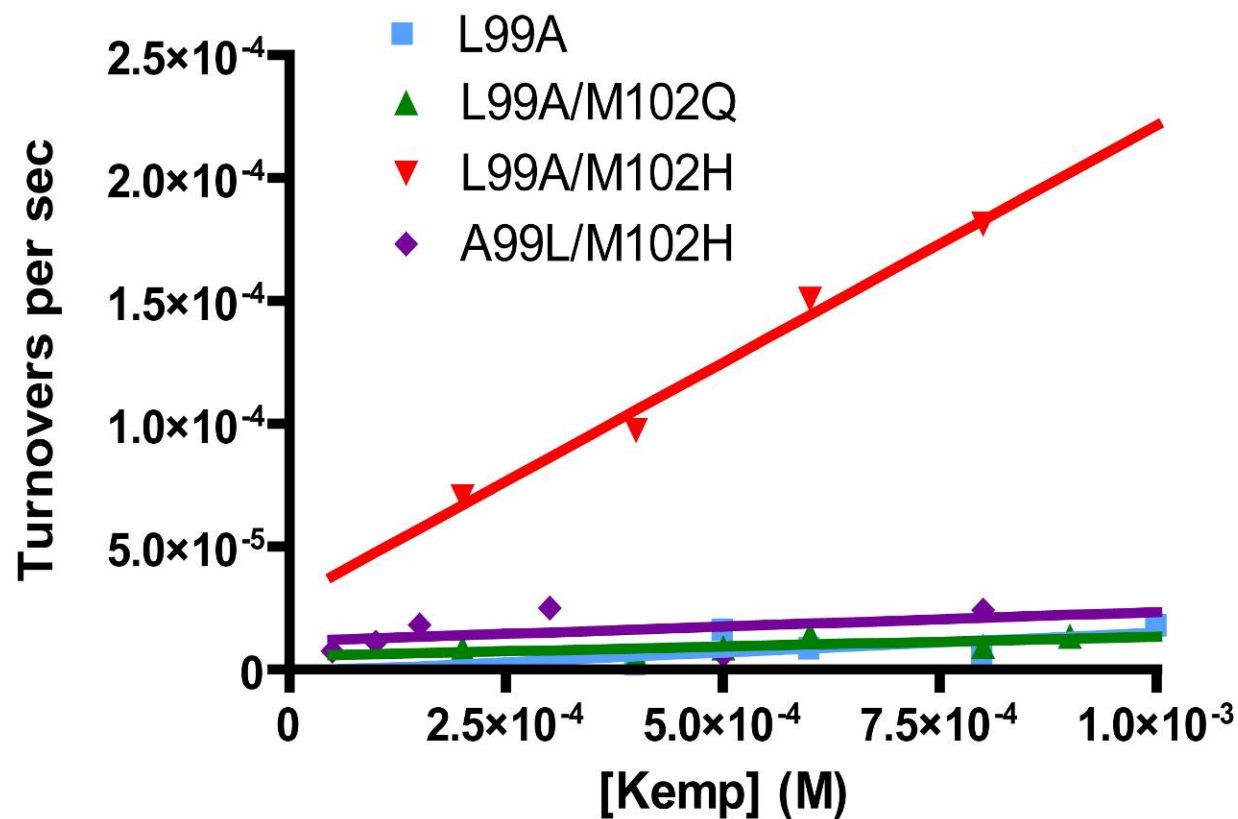
Figure S6: Comparison of the backbone structures of the starting cavity L99A (from PDB ID 181L, shown in orange with its ligand benzene shown in red to locate the cavity site) and L99A/M102H† (shown in blue, from this paper). The N-terminal His-tag of L99A/M102H† is visible at the bottom of the figure and is not present in PDB ID 181L. The overall RMSD is 0.604 Å and there is little variation in the position of the backbone atoms visible. RMSD calculated by and figure produced by PyMol.
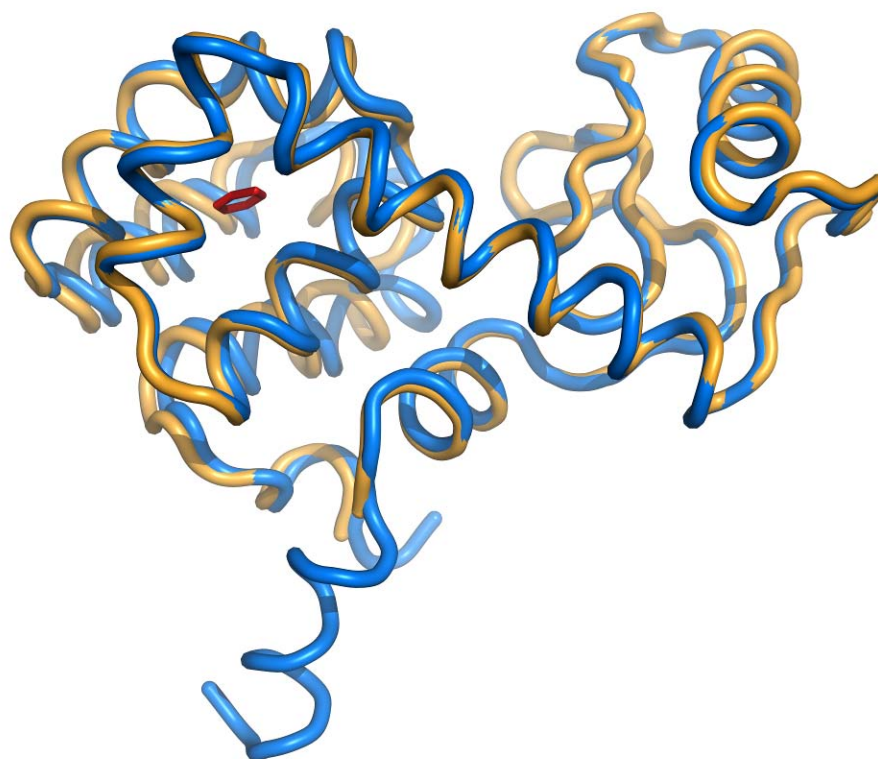
Figure S7: Demonstration that the engineered enzymes catalyze multiple turnovers. Reaction was carried out at pH 5.0 in the standard buffer at RT in the presence of 600 μM Kemp isoxazole using the L99A/M102H†/N68C/A93C construct. The spontaneous rate of Kemp elimination was controlled for by subtracting out the absorbance of a no enzyme control reaction. Turnovers were normalized for the amount of protein present and the initial absorbance after the addition of the enzyme was adjusted to zero to compensate for absorbance present in the assay at the start of the reaction.
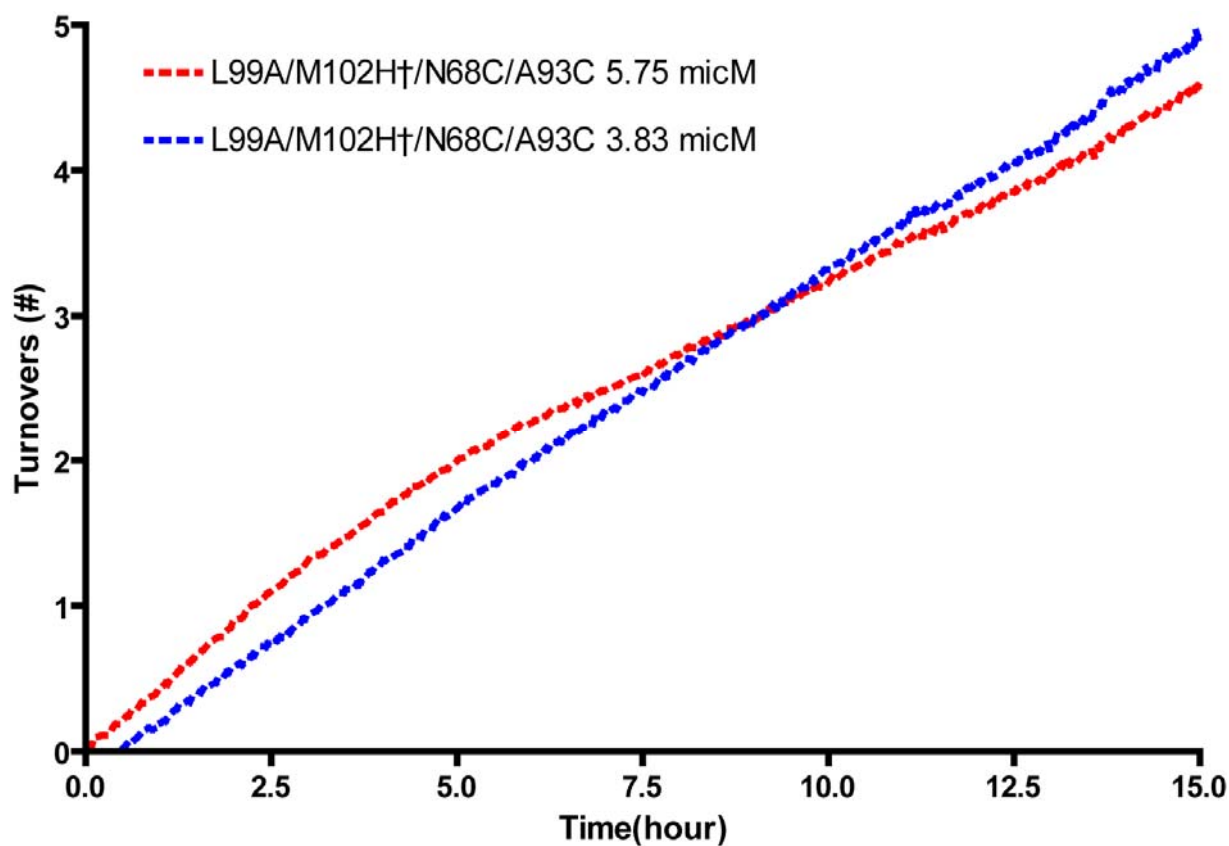
Figure S8: Catalytically competent poses of the ligand and 1,2-benzisoxazole generated by molecular docking. The protein is shown with blue carbons and the crystallographic ligand with white carbons. DOCK poses of ligands are shown with orange carbons. In all cases oxygens are red, nitrogens are blue and sulfurs are yellow. Figure rendered with PyMol. **A)** Highest ranking catalytically competent pose of benzisoxazole generated by molecular docking. This pose was the 4th highest ranked pose of 1,2-benzisoxazole {DOCK score = -14.33 kcal/mol, potential rank #2,693 (0.41%)} but had a smaller RMSD to the crystallographic pose (0.62 Å) than the highest ranked (lowest energy) pose. **B)** Highest ranking catlytically competent pose of the Kemp substrate generated by molecular docking. This pose was ranked 13th among the poses for this molecule and did not score well {RMSD = 1.38 Å for the common atoms, DOCK score = 26.54 kcal/mol, potential rank #96,602 (14.73%)}. However, the highest scoring pose was not well scored either, suggesting that binding of the Kemp substrate may require rearrangement of the receptor structure.
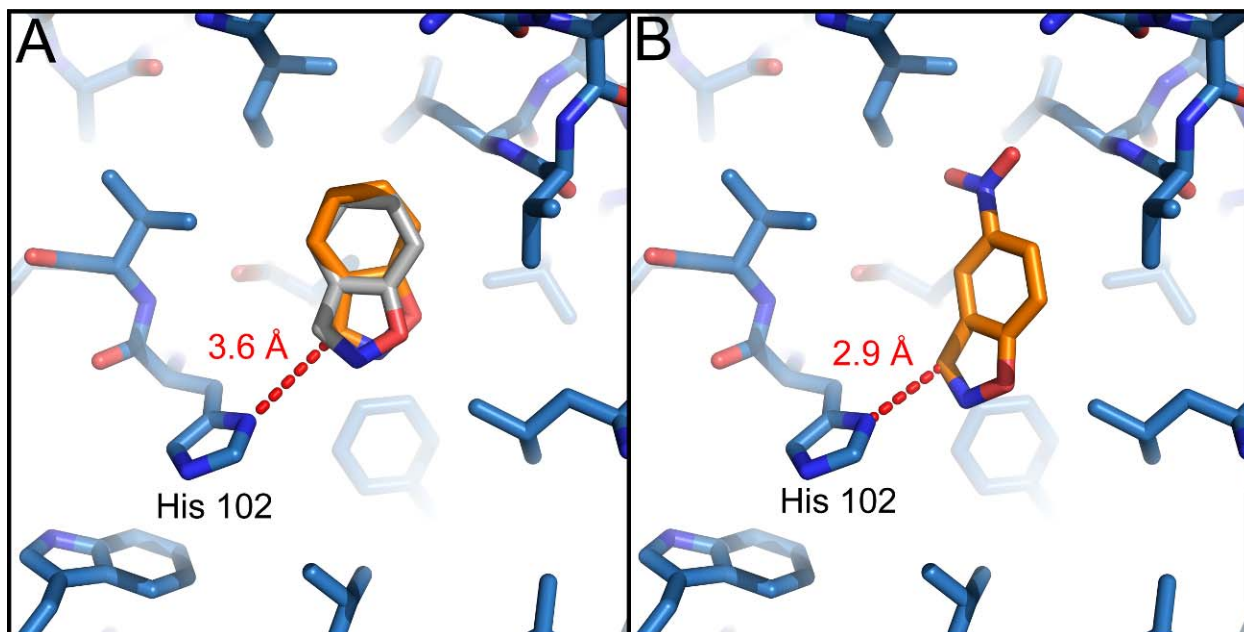
References:
1.   Ho SN, Hunt HD, Horton RM, Pullen JK, & Pease LR (1989) Site-directed mutagenesis by overlap extension using the polymerase chain reaction. *Gene* 77(1):51-59.
2.   Morton A, Baase WA, & Matthews BW (1995) Energetic Origins of Specificity of Ligand-Binding in an Interior Nonpolar Cavity of T4 Lysozyme. *Biochemistry* 34(27):8564-8575.
3.   Kirchhhoff W (1993) EXAM (NIST, Gaithersburg, MD).
4.   Becktel WJ & Schellman JA (1987) Protein Stability Curves. *Biopolymers* 26(11):1859-1877.
5.   Lindemann H & Thiele H (1926) Zur Chemie des Benz-α,β-isoxaols. {On the Chemistry of the α,β-Benzisoxazoles} *Justus Liebigs Annalen der Chemie* 449(1):63-81 (in German).
6.   Ellis KJ & Morrison JF (1982) Buffers of Constant Ionic-Strength for Studying pH-Dependent Processes. *Method Enzymol* 87:405-426.
7.   Rothlisberger D*, et al.* (2008) Kemp elimination catalysts by computational enzyme design. *Nature* 453(7192):190-194.
8.   Kabsch W (2010) XDS. *Acta Crystallogr D* 66:125-132.
9.   Mccoy AJ*, et al.* (2007) Phaser crystallographic software. *J Appl Crystallogr* 40:658-674.
10.   Adams PD*, et al.* (2010) PHENIX: a comprehensive Python-based system for macromolecular structure solution. *Acta Crystallogr D* 66:213-221.
11.   Emsley P, Lohkamp B, Scott WG, & Cowtan K (2010) Features and development of Coot. *Acta Crystallogr D* 66:486-501.
12.   Winn MD, Isupov MN, & Murshudov GN (2001) Use of TLS parameters to model anisotropic displacements in macromolecular refinement. *Acta Crystallogr D* 57:122-133.
13.   Schuttelkopf AW & van Aalten DMF (2004) PRODRG: a tool for high-throughput crystallography of protein-ligand complexes. *Acta Crystallogr D* 60:1355-1363.
14.   Morton A & Matthews BW (1995) Specificity of Ligand-Binding in a Buried Nonpolar Cavity of T4 Lysozyme - Linkage of Dynamics and Structural Plasticity. *Biochemistry* 34(27):8576-8588.
15.   Chen VB*, et al.* (2010) MolProbity: all-atom structure validation for macromolecular crystallography. *Acta Crystallogr D* 66:12-21.
16.   DeLano WL The PyMOL Molecular Graphics System (Schrödinger, LLC).
17.   Debler EW*, et al.* (2005) Structural origins of efficient proton abstraction from carbon by a catalytic antibody. *P Natl Acad Sci USA* 102(14):4984-4989.
18.   Privett HK*, et al.* (2012) Iterative approach to computational enzyme design. *P Natl Acad Sci USA* 109(10):3790-3795 .
19.   Khersonsky O*, et al.* (2011) Optimization of the *In Silico*-Designed Kemp Eliminase KE70 by Computational Design and Directed Evolution. *J Mol Biol* 407(3):391-412.
20.   Khersonsky O*, et al.* (2010) Evolutionary optimization of computationally designed enzymes: Kemp eliminases of the KE07 series.*J Mol Biol* 396(4):1025-1042.
21.   Khersonsky O*, et al.* (2012) Bridging the Gaps in Design Methodologies by Evolutionary Optimization of the Stability and Proficiency of Designed Kemp Eliminase KE59. *P Natl Acad Sci USA* 109(26):10358-10363.
22.   Korendovych IV*, et al.* (2011) Design of a switchable eliminase. *P Natl Acad Sci USA* 108(17):6823-6827.